# Radiative Heating of High-Level Clouds and its Impacts on Climate

**Kerstin Haslehner[1], Blaž Gasparini[1], and Aiko Voigt[1]**

[1]Department of Meteorology and Geophysics, University of Vienna, Vienna, Austria

**Key Points:**

- We create a method that accurately diagnoses the radiative heating of high-level clouds by removing artificial cloud boundaries.
- The radiative interactions of high-level clouds strengthen the eddy-driven jet stream.
- They reduce precipitation in the tropics and lower midlatitudes, but have no substantial effect on the tropical circulation.

Corresponding author: Kerstin Haslehner, `kerstin.haslehner@univie.ac.at`

**Abstract**

The interactions of clouds with radiation influence climate. Many of these impacts appear to be related to the radiative heating and cooling from high-level clouds in the upper troposphere, but few studies have explicitly tested this. Here, we use simulations with the ICON-ESM global atmosphere model to understand how high-level clouds through their radiative heating and cooling of the atmosphere, influence the large-scale atmospheric circulation and precipitation in the present-day climate. We introduce a new method to diagnose the radiative heating of high-level clouds: we use a temperature threshold of -35°C to define high-level clouds and also include the lower parts of these clouds at warmer temperatures. The inclusion of the lower cloud parts circumvents the creation of artificial cloud boundaries and strong artificial radiative heating at the temperature threshold. To isolate the impact of high-level clouds, we analyze simulations with active cloud-radiative heating, with the radiative heating from high-level clouds set to zero, and with the radiative heating from all clouds set to zero. We show that the radiative interactions of high-level clouds warm the troposphere and strengthen the eddy-driven jet streams, but have no impact on the strength of the Hadley circulation and the latitude of the Intertropical Convergence Zone. Consistent with their positive radiative heating and energetic arguments, high-level clouds reduce precipitation throughout the tropics and lower midlatitudes. Overall, our results confirm that the radiative interactions of high-level clouds have important impacts on climate and highlight the need for better representing their radiative interactions in models.

**Plain Language Summary**

The interactions of clouds with electromagnetic radiation shape the climate of our planet by causing heating and cooling within the atmosphere. Here, we use a computer model of the atmosphere to investigate how high-level clouds interact with radiation and thereby influence climate. We find that the interactions of high-level clouds with radiation strengthen the winds in the midlatitudes and reduce rainfall in many regions. This confirms that high-level clouds are important for our climate, and highlights the need to improve their representation in our models of the atmosphere and climate.

# 1 Introduction

The interactions of clouds with radiation are crucial for shaping the present and future climate of Earth (Y. Li et al., 2015; Voigt & Shaw, 2016; Voigt et al., 2021). In this work, we focus specifically on high-level clouds and study their impact on the present-day climate.

High-level clouds are distinct from other clouds. Their impact on Earth's energy budget is small because their warming effect by absorbing outgoing longwave radiation from lower parts of the atmosphere (Hong et al., 2016; Matus & L'Ecuyer, 2017) is nearly offset by their cooling effect due to the reflection of solar radiation (L'Ecuyer et al., 2019). Inside the atmosphere, the radiative interactions of high-level clouds have a warming effect that is strongest in tropical regions. This is different from low-level clouds, whose radiative interactions cool the atmosphere as well as the climate system as a whole. High-level clouds form predominantly in the tropics as a result of deep convection, in the storm track regions because of synoptic ascent and due to orographic forcing (Wernli et al., 2016; Gryspeerdt et al., 2018; Krämer et al., 2020). Therefore, their radiative interactions lead to distinct patterns of diabatic heating and cooling within the atmosphere that can influence atmospheric circulations (Dinh et al., 2023).

High-level clouds pose substantial challenges to models. The ice formation mechanisms and dynamical processes that generate high-level clouds are not completely understood and not well represented by the microphysical parameterizations in current global

climate models (Kärcher, 2017; Heymsfield et al., 2017; Morrison et al., 2020). Their interaction with radiation is complicated due to temperature- and process-dependent ice crystal shapes and their complexity (Lawson et al., 2019; Järvinen et al., 2023). As a result, simulated high-level clouds differ substantially between models as well as between models and observations (Lauer et al., 2023). Recently, Voigt et al. (2023) highlighted model differences in cloud-radiative heating in the upper troposphere, extending the findings of Voigt et al. (2019); Cesana et al. (2019) and Johansson et al. (2021).

Previous work studied the impact of cloud-radiative interactions on the present-day circulation and precipitation by means of the Clouds On-Off Klimate Model Intercomparison Experiment approach (COOKIE; Stevens et al., 2012; Harrop et al., 2023) that compares simulations with and without active cloud-radiative heating. Using this approach it was shown that cloud-radiative interactions reduce tropical precipitation (Y. Li et al., 2015; Harrop & Hartmann, 2016; Albern et al., 2018), narrow the Intertropical Convergence Zone (ITCZ) (Harrop & Hartmann, 2016; Watt-Meyer & Frierson, 2017; Albern et al., 2018; Dixit et al., 2018), strengthen the Hadley cell (Harrop & Hartmann, 2016; Watt-Meyer & Frierson, 2017; Albern et al., 2018), increase the strength of the eddy-driven jet stream (Y. Li et al., 2015), and impact the intensity of tropical cyclones (Ruppert et al., 2020) and the life cycle of tropical anvil clouds (Hartmann et al., 2018; Gasparini et al., 2022). While some of these studies have pointed to an important role of high-level clouds, few attempts have been made to quantify the impact of high-level clouds.

Since high-level clouds are distinct from other clouds and current climate models have difficulties in representing them, we aim to assess their role for the present-day climate through adapted COOKIE simulations. Our work builds on Lohmann and Roeckner (1995) and Dixit et al. (2018). Lohmann and Roeckner (1995) used a fixed pressure threshold to study the impact of the interactions of high-level clouds with longwave radiation. Dixit et al. (2018) investigated the radiative impact of high-level clouds on the ITCZ width in aquaplanet simulations. Here, we perform simulations with realistic boundary conditions and study both the longwave and shortwave impacts.

We address two research questions:

1. How should high-level clouds be defined to study their cloud-radiative heating?
2. What is the radiative impact of high-level clouds on the present-day climate in terms of atmospheric temperature, circulation and precipitation?

## 2 Methodology

### 2.1 ICON-ESM Atmosphere Model and Simulation Setup

We use ICON-ESM (ICOsahedral Non-hydrostatic-Earth System Model) version 1.0 as described by Jungclaus et al. (2022). ICON-ESM is based on the unified ICON modeling framework for weather and climate, and is designed for the study of the past, present, and future climates of Earth. We perform our model simulations with a horizontal grid resolution of R2B04, which corresponds to about 160 km, and 47 atmospheric levels. The model is coupled to the radiation scheme PSrad (Pincus & Stevens, 2013), the convective parameterization based on Tiedtke (1989), a 1-moment cloud microphysics scheme (Lohmann & Roeckner, 1996), and the cloud cover scheme by Sundqvist et al. (1989). The model time step is 15 minutes, except for the radiation scheme, which uses a time step of 90 minutes.

We perform ICON-ESM simulations with prescribed monthly-mean sea-surface temperatures and sea ice cover. This allows us to focus on the cloud-radiative heating within the atmosphere. The simulations are run for 31 years; we discard the first year from the analysis to exclude the spin up effects. Our simulation setup is similar to the AMIP pro-

tocol, except for the fact that sea surface temperatures and sea ice cover are prescribed to their climatological averages from the years 1979 to 2008.

## 2.2 Cloud-radiative Effect and Cloud-radiative Heating

The cloud-radiative effect (CRE) quantifies the influence of clouds on the radiative fluxes at the top of atmosphere (TOA) and the surface (SFC). As such, CRE are helpful to understand the contribution of cloud-radiative interactions to the energy balance of the Earth and the surface, respectively. CRE is defined as the difference between all-sky and clear-sky radiative fluxes $F$:

$$\mathrm{CRE} = F^{all-sky} - F^{clear-sky}, \tag{1}$$

where $F$ is defined as positive downward. The unit of CRE is $W/m^2$. Positive values mean a radiative heating, while negative values mean a radiative cooling. The difference between the CRE at the TOA and SFC is the cloud-radiative effect within the atmosphere (ATM):

$$\mathrm{CRE_{ATM}} = \mathrm{CRE_{TOA}} - \mathrm{CRE_{SFC}}. \tag{2}$$

$\mathrm{CRE_{ATM}}$ is the vertical integral of the energy gained or lost by an atmospheric column due to cloud-radiative interactions.

We define the CRE of high-level clouds as the difference between the all-sky radiative fluxes and the radiative fluxes that would occur if high-level clouds did not interact with radiation:

$$\mathrm{highCRE} = F^{all-sky} - F^{no-hlc}. \tag{3}$$

The superscript $no-hlc$ indicates transparent high-level clouds. The definition is equally valid at the TOA, SFC and within the atmosphere. We discuss the definition of high-level clouds and the technical implementation in Section 3.

To characterize the vertical structure of cloud-radiative interactions within the atmosphere, we use the cloud-radiative heating:

$$\mathrm{CRH} = \left.\frac{\partial T}{\partial t}\right|_{rad}^{all-sky} - \left.\frac{\partial T}{\partial t}\right|_{rad}^{clear-sky} = -\frac{g}{\rho c_p}\frac{\partial(F^{all-sky} - F^{clear-sky})}{\partial p}, \tag{4}$$

where $\left.\frac{\partial T}{\partial t}\right|_{rad}^{all-sky}$ is the all-sky radiative heating rate, $\left.\frac{\partial T}{\partial t}\right|_{rad}^{all-sky}$ is the clear-sky heating rate, $g$ is the gravitational acceleration, $c_p$ is the specific heat capacity of moist air at constant pressure and $p$ is the pressure. Different to Eq. 1, the radiative fluxes $F$ are a function of pressure and so are not only at the TOA and SFC but all altitudes.

Analogously to highCRE, we define the cloud-radiative heating from high-level clouds as:

$$\mathrm{highCRH} = \left.\frac{\partial T}{\partial t}\right|_{rad}^{all-sky} - \left.\frac{\partial T}{\partial t}\right|_{rad}^{no-hlc} = -\frac{g}{c_p}\frac{\partial(F^{all-sky} - F^{no-hlc})}{\partial p}. \tag{5}$$

Our assessment of the radiative effects of high-level clouds uses the all-sky atmosphere as reference. One could also choose the clear-sky atmosphere as a reference and use the difference in radiative fluxes between an atmosphere in which only high-level clouds interact with radiation and a clear-sky atmosphere. Haslehner (2023) showed that the overall results are independent of this choice. In our view the all-sky reference is physically more meaningful: the all-sky atmosphere is a state that is actually realized by the model, whereas the clear-sky atmosphere is a hypothetical state that the model never attains.

## 2.3 Simulations with Transparent Clouds: COOKIE and highCOOKIE

We follow the method of the Clouds On-Off Klimate Model Intercomparison Experiment (COOKIE; Stevens et al., 2012) to study the cloud-radiative impact on the present-day climate. In the COOKIE framework, a simulation with active CRH, called the "clouds

on" simulation, is compared with a simulation in which all clouds are made transparent to radiation, the "clouds off" simulation. Clouds are made transparent by setting cloud fraction as well as cloud liquid and ice mass to zero for the radiation calculation. In the "clouds off" simulation, clouds are still simulated and can generate latent heating and precipitation. COOKIE is useful to understand how cloud-radiation interactions impact the present-day climate (Voigt & Albern, 2019).

To specifically study the impact of high-level clouds, we extend the COOKIE method and conduct a third "high-level clouds off" simulation in which only high-level clouds are made transparent to radiation.

In the following, COOKIE means the difference between the "clouds on" and "clouds off" simulations, and highCOOKIE means the difference between the "clouds on" and "high-level clouds off" simulations.
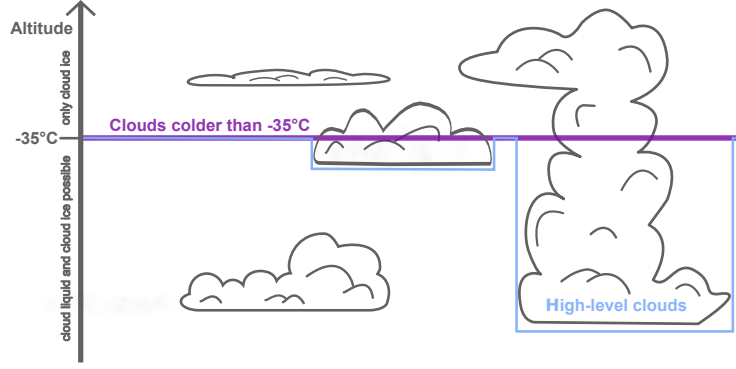
## 3  Definition of High-Level Clouds

We begin with the problem of how to define high-level clouds. Previous studies have defined high-level clouds based on threshold values for pressure or temperature (Lohmann & Roeckner, 1995; Dixit et al., 2018). However, as we will show, this creates artifacts in cloud-radiative heating, because of which we propose an alternative definition.

A simple definition of high-level clouds considers all clouds that are colder than a certain temperature or pressure threshold. In ICON-ESM, only ice clouds can exist at temperatures below -35°C, while at higher temperatures cloud liquid water is possible (Lohmann & Roeckner, 1996). Therefore, the appropriate temperature threshold is -35°C; the same threshold was used in Gasparini et al. (2017) and Gasparini et al. (2020). This definition of high-level clouds works well when the cloud base is colder than -35°C. Yet, it causes problems when parts of a cloud extend further below to warmer regions of the atmosphere. In this case, only the upper colder parts of the cloud are considered as high-level clouds, while the warmer lower parts are considered as non-high-level clouds. The result is a temperature-based artificial "slicing" of the cloud into two parts. The purple line in Fig. 1 illustrates this simple definition.
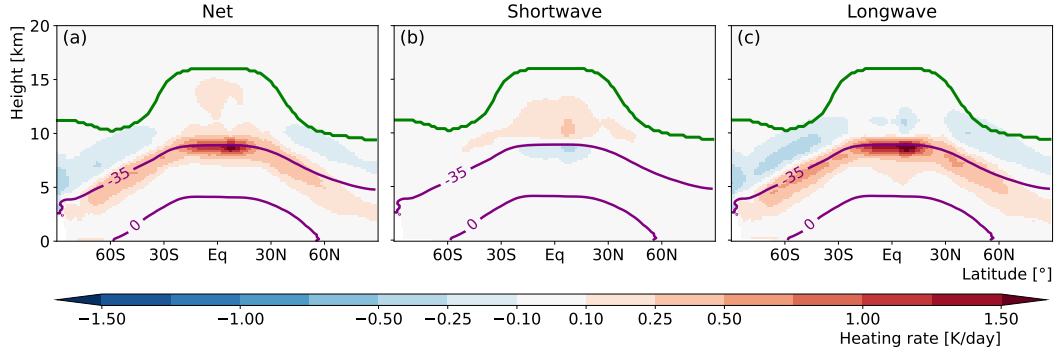
The "cloud slicing" results in strong heating rates in the vicinity of the temperature threshold, as is illustrated in Fig. 2. The heating rates occur because the slicing creates cloud tops and hence strong longwave emission at the temperature threshold. The heating rates around the temperature threshold are artificial and bear no resemblance to the actual CRH, which will be discussed later and is shown in Fig. 5. The artificial heating also occurs when clouds are separated based on a pressure threshold, as shown in the appendix of Voigt and Shaw (2016).

We therefore propose an alternative definition for high-level clouds. At each time step of the radiation scheme, we consider all clouds colder than -35°C as high-level clouds and additionally include those clouds that exist at warmer temperatures and are vertically connected to clouds colder than -35°C. This is illustrated by the blue line in Fig. 1. In this way, no artificial cloud tops and no artificial heating rates are created. Section 4.2 discusses the high-level cloud-radiative heating following this definition.

Fig. 3 shows the climatological distribution of high-level clouds in ICON-ESM. High-level clouds occur throughout the tropics and the mid and high latitudes, and are less pronounced in the subtropics. The most high-level clouds occur over Antarctica. In the Southern Hemisphere high-level clouds extend well into the stratosphere. The two definitions of high-level clouds differ in the mixed-phase cloud regime, since the cloud parts at temperatures warmer than the -35°C threshold are included in our adapted definition but not in the simple definition. Most of these warmer cloud parts are located in the regions of tropical deep convection and the midlatitude storm tracks. Our definition clas-

**Figure 1.** Comparison of two ways to define high-level clouds. The simple definition based purely on the -35°C temperature threshold is shown by the purple line. The definition that includes lower cloud parts is shown by the blue line. The latter definition is used in the manuscript. The blue line follows the -35°C isotherm, yet if a high-level cloud has its base at a warmer temperature, its lower parts are also taken into account.
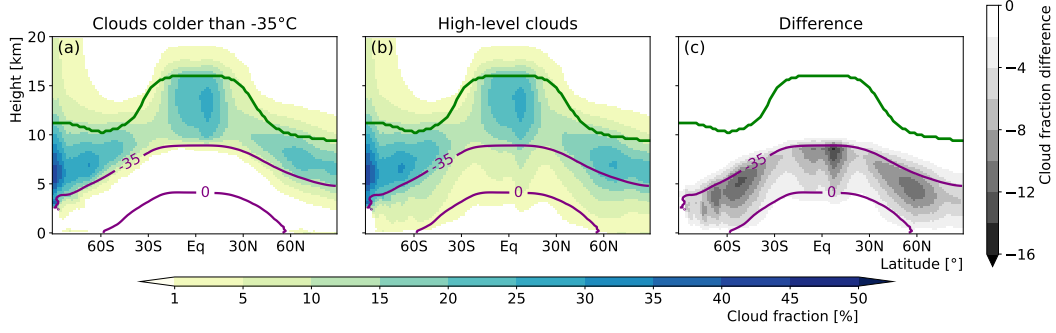


**Figure 2.** Zonal-mean annual-mean radiative heating by high-level clouds for the simple definition of high-level clouds with a purely temperature based criterion for net, shortwave and longwave radiation. Purple lines show the -35°C and 0°C isotherms. The green line depicts the thermal tropopause.

sifies also lower parts of towering deep convective cumulus, with cloud bases at temperatures substantially higher than 0°C clouds as high-level clouds. However, this does not happen often, as seen by the low fraction of high-level clouds in the lower troposphere in Fig. 3 b.

We note that the large artificial heating at the temperature threshold (Fig. 2) would also be avoided by only considering clouds with a cloud base at temperatures below -35°. However, such clouds are very thin and do not substantially impact the radiative budget in ICON-ESM. We therefore do not use such a definition.

## 4 Radiative Effects and Radiative Heating of High-Level Clouds

This section assesses the contribution of high-level clouds to radiative effects and radiative heating. To this end, we analyse the "clouds on" simulation and use the diagnostics described in Sects. 2.

**Figure 3.** Zonal-mean annual-mean high-level cloud fraction for the two definitions of high-level clouds. Panel a shows the simple definition, panel b the definition used in the manuscript, and panel c the difference. Purple lines show the -35°C and 0°C isotherms. The green line depicts the tropopause.

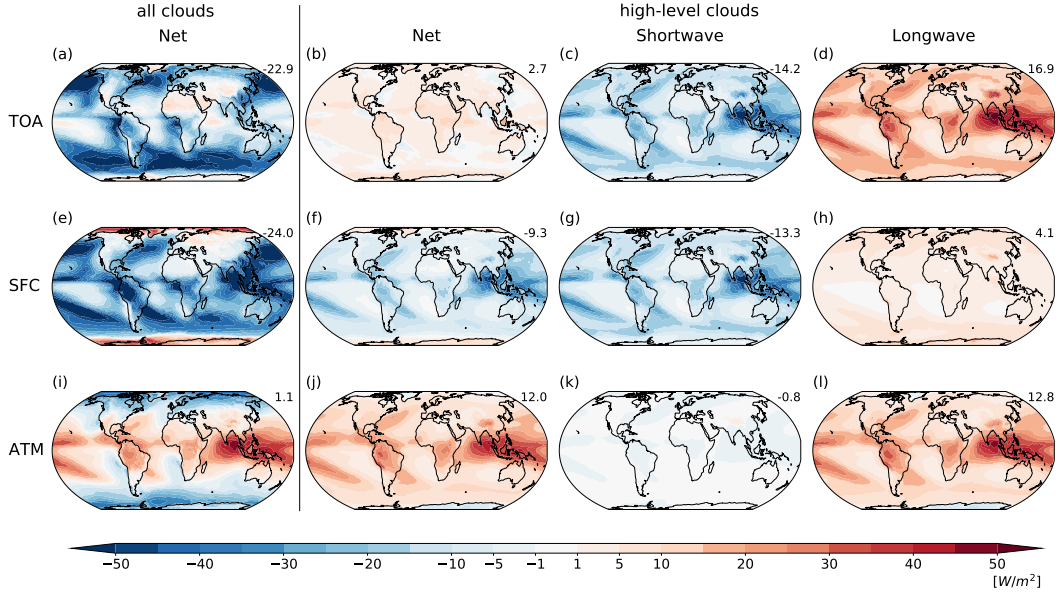#### 4.1 Radiative effects at TOA, SFC and ATM

The impact of cloud-radiative interactions on the energy budget at the TOA, the surface and inside the atmosphere can be characterized by CRE. The net CRE from all clouds is shown in the left row of Fig. 4, the CRE from high-level clouds is shown in the other rows of the figure for net, shortwave and longwave radiation.

At the TOA, the net CRE is negative in the global mean and in most regions, consistent with observations from CERES EBAF (Loeb et al., 2018). Strong negative values occur over the mid-latitude oceans and the cold upwelling regions of the subtropical oceans as a result of extensive low-level clouds (Fig. 4 a). In contrast, the net high-CRE from high-level clouds is weak and mostly positive at the TOA (Fig. 4 b). The net highCRE is near neutral because of the compensation between strong negative shortwave and positive longwave effects (Fig. 4 c and d), whose spatial patterns reflect the distribution of high-level clouds.

At the surface, the net CRE is negative except at high latitudes (Fig. 4 e), consistent with observations from CERES EBAF-SFC (Kato et al., 2018; Voigt et al., 2021). The net highCRE from high-level clouds follows the same spatial pattern as net CRE from all clouds (Fig. 4 f), yet with a weaker magnitude. High-level clouds cool the surface (Fig. 4 g) due to their shortwave effect that dominates the net highCRE. In the longwave, high-level clouds slightly warm the surface (Fig. 4 h).

Inside the atmosphere, the net CRE is positive at low latitudes and negative at high latitudes (Fig. 4 ). The meridional CRE contrast reflects the meridional contrast in high- and low-level clouds (Voigt et al., 2021). Consistent with this, the net highCRE from high-level clouds is strongly positive in the tropics and near zero in high latitudes. The net highCRE is dominated by the longwave effect, with the shortwave effect contributing little (Fig. 4 k and l). Over the ice sheets of Greenland and Antarctica, the longwave highCRE is slightly negative.

Previous work estimated CRE of different cloud types from satellite measurements (Hong et al., 2016; Matus & L'Ecuyer, 2017; Oreopoulos et al., 2017). These studies defined cloud types in different ways and in ways that are different from our definition of high-level clouds. Nevertheless, the patterns of highCREs simulated by ICON-ESM overall agree with the CRE estimates for ice clouds by Hong et al. (2016) and Matus and L'Ecuyer (2017). Moreover, the global averages of simulated highCRE are consistent with Oreopoulos

**Figure 4.** Net CRE of all clouds and net, shortwave, and longwave highCRE of high-level clouds at the TOA, the surface and inside the atmosphere. For each subplot, the global mean is shown in the upper right.
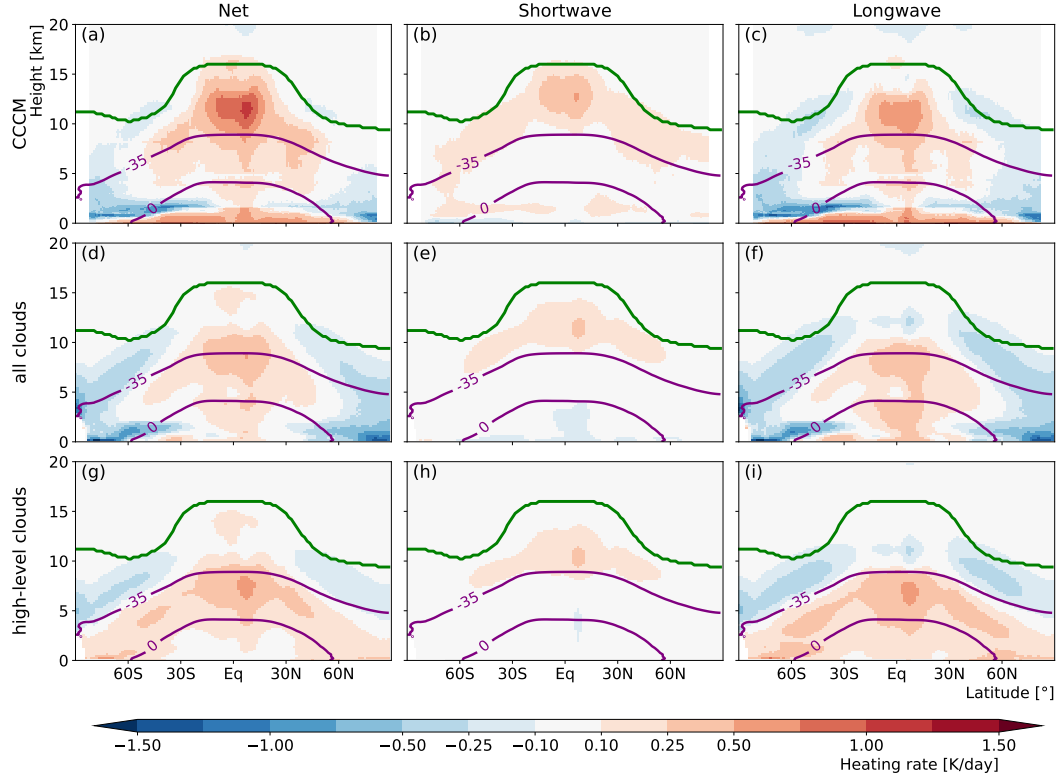
et al. (2017), although ICON-ESM exhibits somewhat smaller values compared to the observations.

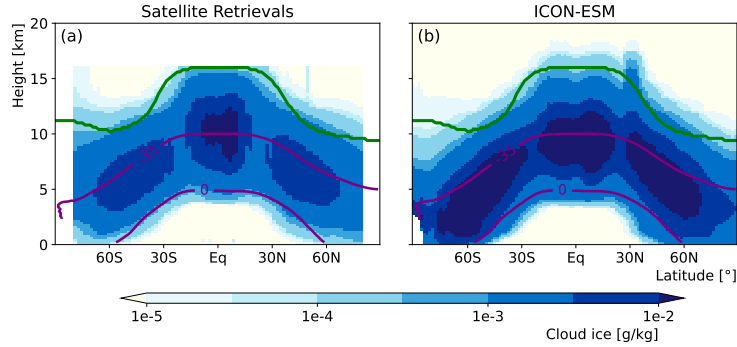## 4.2 Radiative Heating of High-Level Clouds

Clouds create radiative heating inside the atmosphere that varies in the vertical dimension. The vertical variations are not captured by the CRE inside the atmosphere, because of which we now consider the cloud-radiative heating CRH. To assess how well ICON-ESM captures the zonal-mean time-mean CRH, we compare the CRH from all clouds with the RelD1 product of CERES-CALIPSO-CloudSat-MODIS (CCCM) (Kato et al., 2021). We use the CCCM estimate for CRH obtained from daytime radiative fluxes for the period of 2007 to 2010 (Ham et al., 2017). Fig. 5 shows the CRH from CCCM as well as from all clouds and high-level clouds in ICON-ESM.

The net CRH from CCCM is strongest in the tropical upper troposphere and near the surface (Fig. 5 a). Strong heating occurs in the tropical upper troposphere as a result of high-level clouds; strong cooling occurs in the lower troposphere near the top of low-level clouds. The shortwave CRH is largest in the tropical upper troposphere (Fig. 5 b). Longwave CRH also shows a strong heating in the tropical upper troposphere (Fig. 5 c). and is the main contributor to the net CRH in the mid- to lower troposphere.

Compared to CCCM, the net CRH of ICON-ESM (Fig. 5 d) is less pronounced near the surface since ICON-ESM lacks low-level clouds (Jungclaus et al., 2022). The net CRH is also weaker compared to CCCM in the tropical upper troposphere. This underestimation does not result from a lack of high-level tropical clouds (Fig. 3; Jungclaus et al., 2022). Instead tropical cloud ice is overestimated at temperatures around -35°C compared to observations (Fig. 6; Lauer et al., 2023), leading to optically thick high-level clouds and hence longwave cooling instead of heating. The cause of this overestimation of cloud ice might be that high-level clouds in ICON-ESM are at too low altitudes. In the mid-

**Figure 5.** Zonal-mean annual-mean radiative heating of all clouds and of high-level clouds for net, shortwave and longwave radiation. The first row shows the observational estimate by CCCM. The second row shows the radiative heating of all clouds in ICON-ESM, whereas the third row shows the radiative heating of high-level clouds. Purple lines show the -35°C and 0°C isotherms. The green line depicts the tropopause.



**Figure 6.** Zonal-mean annual-mean cloud ice (a) in the CloudSat and CALIPSO observations and (b) in ICON-ESM. The green line depicts the tropopause. The observational data is taken from J.-L. F. Li et al. (2012).

latitudes, net CRH in the upper troposphere is somewhat stronger in ICON-ESM than in CCCM.

The upper-tropospheric CRH of all clouds is well captured by the highCRH from high-level clouds (Fig. 5, middle and lower rows). At temperatures above -35°C, i.e., in

the mid- to lower troposphere, the net highCRH is positive everywhere. This is different from the net CRH of all clouds because only the cloud bases of high-level clouds are taken into account and low clouds are not considered. This means that the highCRH effectively removes the radiative heating of low-level clouds. The bases of high-level clouds are not concentrated at the -35°C temperature threshold, as opposed to the simple definition of high-level clouds. This eliminates the artificial heating at -35°C that occurs for the simple definition (Fig. 2) and shows that upper-tropospheric CRH is best studied by using the definition of high-level clouds that includes the lower cloud parts at warmer temperatures.

ICON-ESM has a much weaker CRH in the tropical upper troposphere compared to the observational estimate by CCCM and other CMIP6 models (Voigt et al., 2023). Therefore, the radiative impacts of high-level clouds on the circulation and precipitation that are examined in the following section should be considered as a lower bound of their effect in the real atmosphere.

## 5 The Impacts of Radiative Heating of High-Level Clouds on Climate

The previous section diagnosed the radiative interactions of high-level clouds in the present-day climate as simulated by ICON-ESM. In this section, we study how the radiative interactions of high-level clouds affect climate in terms of temperatures, circulation and precipitation, and how these impacts compare to the radiative impacts of all clouds. To this end, we make use of the "clouds on", "clouds off" and "high-level clouds off" simulations. Throughout the section, COOKIE means "clouds on" - "clouds off", and highCOOKIE means "clouds on" - "high-level clouds off".
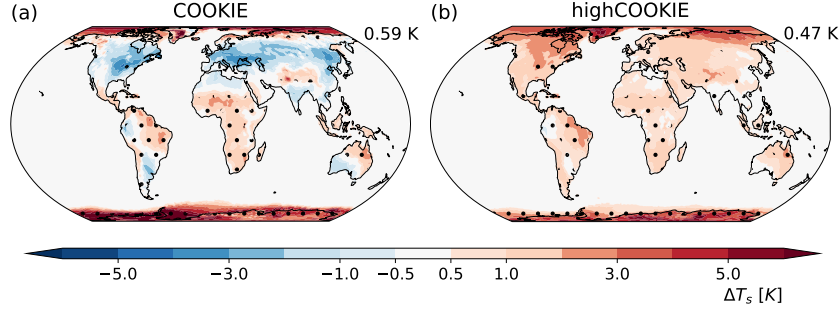
### 5.1 Surface and Atmospheric Temperature Change

When clouds are made transparent to radiation in AMIP-style simulations with prescribed sea-surface temperatures, the temperature of the land and sea-ice surface can still change. For both COOKIE and highCOOKIE, surface temperatures change by more than 1 K over many land regions in the annual mean (Fig. 7). Ideally, one would want to eliminate such surface temperature changes as they might mask some mechanisms through which the cloud-radiative heating of the atmosphere affects climate (Webb et al., 2017; Harrop et al., 2023). In highCOOKIE, the surface temperature changes are smaller than in COOKIE in most regions as well as in the global mean. Moreover, they have the same sign in highCOOKIE in all regions, while COOKIE shows substantial land cooling in the midlatitudes of the Northern Hemisphere and warming in many other regions. Overall, highCOOKIE is therefore less affected by surface temperature changes than COOKIE.

The cloud-radiative impact on tropospheric temperatures in highCOOKIE and COOKIE closely mimics the spatial pattern of highCRH and CRH, respectively (Fig. 8), and shows little seasonal variability. The warming of the tropical upper troposphere is very similar in highCOOKIE and COOKIE, showing that high-level clouds dominate the temperature impact in this region. The entire troposphere warms in highCOOKIE, consistent with Lohmann and Roeckner (1995). In COOKIE, the northern mid and high latitudes experience a cooling that is strongest in boreal summer. This is different to the simulations of Y. Li et al. (2015) with the IPSL-CM5A-LR model, which showed no tropospheric cooling. In fact, the temperature impact in the COOKIE simulations of Y. Li et al. (2015) is similar to our highCOOKIE simulations, suggesting that high-level clouds dominate the overall cloud impact in their IPSL-CM5A-LR simulations.

Stratospheric temperatures decrease in the tropics and the Southern Hemisphere mid-latitudes in both highCOOKIE and COOKIE. This is consistent with clouds reducing the upwelling longwave radiation (Harrop & Hartmann, 2016), with possible further contributions from stratospheric circulation changes (Y. Li et al., 2015; Harrop & Hart-

**Figure 7.** The impact of cloud-radiative interactions on annual-mean surface temperatures for (a) all clouds diagnosed by COOKIE and (b) high-level clouds diagnosed by highCOOKIE. The global mean root mean square for surface temperature changes is given in the upper right of each panel. The stippling indicates statistically significant changes according to the Student's t-test using the false discovery rate method at a 10% level following Wilks (2016).

mann, 2016). Over the high latitudes in the Northern Hemisphere, stratospheric temperatures increase in highCOOKIE and decrease in COOKIE. The overall stratospheric cooling in highCOOKIE and COOKIE agrees with Lohmann and Roeckner (1995); Y. Li et al. (2015) and Harrop and Hartmann (2016), apart from the high latitude warming in the Northern Hemisphere in highCOOKIE.
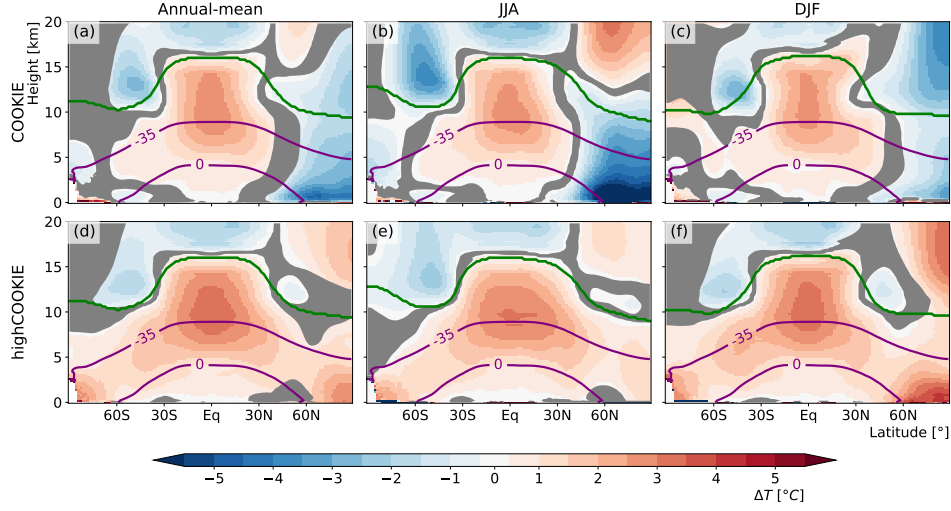
### 5.2 Zonal Wind Change in the Extratropics

We now study changes in the zonal winds and eddy-driven jets caused by cloud-radiation interactions. These changes are related to the changes in atmospheric temperature through the thermal wind balance. For each hemisphere, we determine the position of the eddy-driven jet as the latitude of the maximum zonal-mean zonal wind speed at 700 hPa. To account for effects of the model grid, we use a quadratic fit following Barnes and Polvani (2013). We calculate the strength of the eddy-driven jet from the zonal-mean zonal wind at the jet position. The wind changes are shown in Fig. 9; the changes in the jet metrics are listed in Tab. 1.

Cloud-radiative interactions have a clear impact on the jet strength. In COOKIE, the midlatitude zonal wind and the jet strength decrease in the Southern Hemisphere but increase in the Northern Hemisphere in the annual mean. The annual-mean signal is dominated by the change in the respective summer season, i.e., DJF for the Southern Hemisphere and JJA for the Northern Hemisphere.

Whereas the wind impact from all clouds differs between the hemispheres, the impact of high-level clouds is almost symmetric with respect to the equator. In highCOOKIE, the midlatitude zonal wind and the eddy-driven jet strengthen in both hemispheres, with little seasonal variation. While we do not pursue a detailed dynamical investigation here, the impact of high-level clouds is consistent with an increase of the meridional temperature gradient in the upper troposphere that follows from the high-level cloud radiative heating (Voigt & Shaw, 2016; Butler et al., 2010). The overall increase in the zonal wind in highCOOKIE is consistent with Lohmann and Roeckner (1995). Moreover, the highCOOKIE results are more similar to Y. Li et al. (2015) than the COOKIE results.

The jet position is affected less by cloud-radiative interactions. In the annual mean, cloud-radiative interactions do not lead to statistically significant jet shifts for neither COOKIE nor highCOOKIE. A poleward shift of the Northern Hemisphere jet occurs dur-

**Figure 8.** Annual-mean zonal-mean atmospheric temperature changes due to the radiative interactions of all clouds (COOKIE, first row) and high-level clouds (highCOOKIE, second row). The gray shading indicates statistically insignificant results according to a Student's t-test using the false discovery rate method at a 10% level following Wilks (2016). Purple lines show the -35°C and 0°C isotherms. The green line depicts the thermal tropopause height.
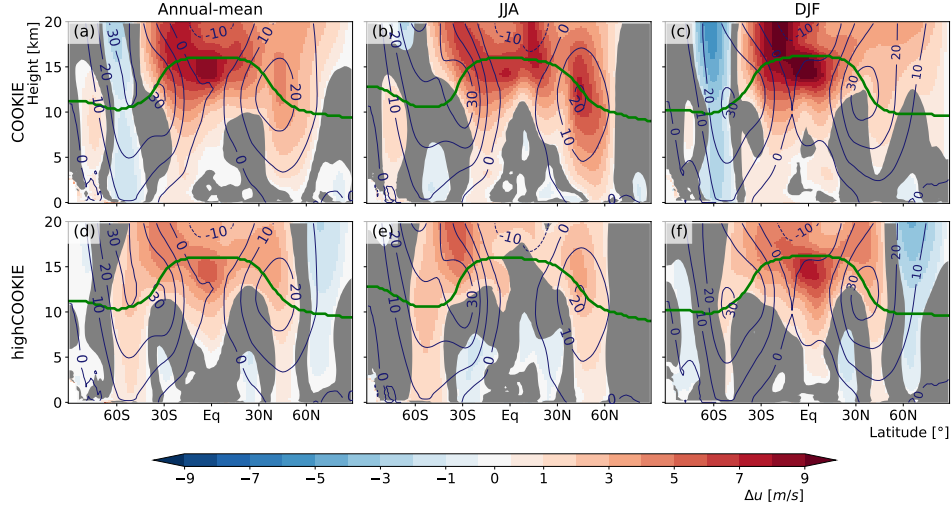
355 ing JJA in COOKIE and highCOOKIE, consistent with a stronger meridional temper-
356 ature gradient (Fig. 8 b and e). An equatorward shift occurs for the Southern Hemisphere
357 jet during DJF in COOKIE (Tab. 1). Overall, however, the cloud-radiative impact on
358 the jet position is small for both highCOOKIE and COOKIE. The small impact is likely
359 a consequence of the opposing effects of tropical and extratropical CRH that were iden-
360 tified by Watt-Meyer and Frierson (2017), and is not surprising given that Voigt et al.
361 (2021) found no robust jet shifts in COOKIE simulations with 5 models.

|  | jet strength in m s$^{-1}$ | | | jet position in deg lat | | |
|---|---|---|---|---|---|---|
|  | annual | JJA | DJF | annual | JJA | DJF |
| NH COOKIE | **0.8** | **1.4** | **0.4** | 0.6 | **4.0** | -1.2 |
| SH COOKIE | **-1.3** | **-0.8** | **-1.6** | 0.0 | 1.0 | **-1.3** |
| NH highCOOKIE | **0.6** | **0.7** | **0.7** | 0.7 | **1.8** | 0.1 |
| SH highCOOKIE | **0.9** | **1.4** | **0.5** | 0.0 | 1.4 | 0.0 |

**Table 1.** Changes in the jet strength and position due the radiative interactions of all clouds and high-level clouds as diagnosed by COOKIE and highCOOKIE. For the jet shift, positive values indicate a poleward shift in both hemispheres, negative values indicate an equatorward shift. Statistically significant changes according to a Student's t-test with a significance level of 5% are shown in bold.

362 ### 5.3 Tropical Precipitation and Circulation Change

363     In the tropics, radiative cooling of the atmosphere is primarily balanced by con-
364 densational heating. Radiative heating of the tropical upper troposphere by high-level
365 clouds reduces the need for condensational heating and hence is expected to decrease pre-
366 cipitation (Y. Li et al., 2015; Albern et al., 2018). Tropical precipitation is reduced in

**Figure 9.** Zonal-mean zonal wind changes due to cloud-radiative interactions of all clouds (COOKIE, first row) and high-level clouds (highCOOKIE, second row). The gray shading indicates statistically insignificant results according to a Student's t-test using the false discovery rate method at a 10% level following Wilks (2016). Blue contour lines show the zonal wind in the "clouds on" simulation. The green contour depicts the tropopause height in the "clouds on" simulation.
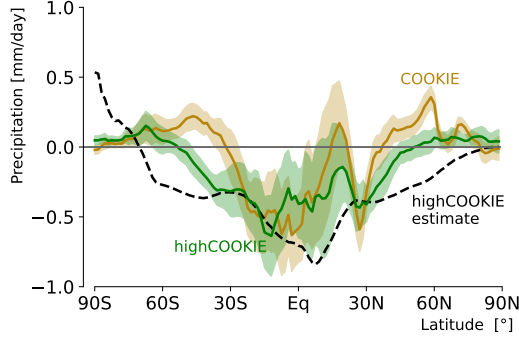
COOKIE (Fig. 10 and Tab. 2), consistent with previous work (Y. Li et al., 2015; Harrop & Hartmann, 2016; Albern et al., 2018). The precipitation reduction is even stronger in highCOOKIE. This confirms that high-level clouds dominate the cloud-radiative impact on tropical precipitation, although one should note that this result might be affected by the underestimation of subtropical and tropical low-level clouds in ICON-ESM (Fig. 3).

The reduction in precipitation due to high-level clouds in the tropics and lower midlatitudes (i.e., equatorward of 50 °N/S) can be understood from the atmospheric energy budget. Neglecting changes in circulation and sensible surface heat fluxes, the precipitation change $dP$ can be predicted by following Pendergrass and Hartmann (2014) as:

$$dP = -\frac{\text{highCRE}_{\text{ATM}}}{L},\tag{6}$$

where $L$ is the latent heat of condensation and $\text{highCRE}_{\text{ATM}}$ is the decrease in the atmospheric radiative cooling due to high-level clouds. Since high-level clouds warm the atmosphere, Eq. 6 predicts a decrease in precipitation at all latitudes apart from Antarctica. The prediction agrees well with the simulated precipitation reduction in highCOOKIE in the subtropics of the Southern Hemisphere. It also captures the general precipitation reduction equatorward of 50 °N/S, although it overestimates the reduction because changes in the surface sensible heat flux and the circulation are neglected.

While the radiative heating from high-level clouds has a clear impact on the amount of tropical precipitation, the tropical circulation is not affected. We quantify this impact through the ITCZ latitude, which we calculate from the latitude centroid of zonal-mean annual-mean precipitation between 20°N/S following Harrop et al. (2018), and the Hadley cell strength, which we define as the maximum of the absolute of the mass stream function between 700 hPa to 200 hPa and between the Equator and 30°N/S for the Northern and Southern Hemisphere, respectively. Tab. 2 lists the changes in the ITCZ position and Hadley strength in COOKIE and highCOOKIE. The ITCZ shifts northward in COOKIE, consistent with Voigt et al. (2021). However, high-level clouds do not cause

**Figure 10.** Changes in annual-mean zonal-mean precipitation due to the radiative interactions of all clouds (yellow) and high-level clouds (green) as diagnosed by COOKIE and highCOOKIE, respectively. The shading shows the annual standard deviation of zonal-mean precipitation in the "clouds on" simulation. The dashed black line shows the precipitation decrease predicted by Eq. 6.

statistically significant changes in the ITCZ position and Hadley cell strength in high-COOKIE. This is in contrast with Lohmann and Roeckner (1995), who found a stronger Hadley cell when high-level clouds are interacting with longwave radiation.

| | $P_t$ | $P_g$ | ITCZ position | $HC_{NH}$ | $HC_{SH}$ |
|---|---|---|---|---|---|
| COOKIE | **-0.33** | **-0.12** | **0.5** | -1 | 9 |
| highCOOKIE | **-0.38** | **-0.23** | 0.3 | -0 | 4 |

**Table 2.** Changes in annual-mean tropical precipitation and circulation due the radiative interactions of all clouds and high-level clouds as diagnosed by COOKIE and highCOOKIE. The change in tropical-mean precipitation $P_t$ is given in mm/day; the change in global-mean precipitation $P_g$ is also given. The tropics are defined as the latitudes between 30°N/S. The change in the ITCZ latitude is given in units of °N. The change in the Hadley cell strength $HC$ is given in $10^9$ kg/s. Statistically significant results according to a Student's t-test with a significance level of 5% are shown in bold.

## 6 Conclusions

In this manuscript, we present a thorough assessment of how high-level clouds affect climate via their radiative heating and cooling in the atmosphere. This required us to solve two problems. First, we clarify how high-level clouds should be defined in the context of radiation. And second, we propose a simulation strategy that specifically targets the radiative heating of high-level clouds. For both problems, we use the simulations of the present-day climate with the ICON-ESM model.

For studies of cloud-radiative heating, the definition of high-level clouds is adapted from existing definitions that are based on fixed pressure or temperature thresholds. We show that artificial cloud tops and artificial radiative heating arise when a purely temperature-based threshold is used. We further show that the artificial heating is removed by including the lower cloud parts at warmer temperatures in the definition of high-level clouds.

Using this definition of high-level clouds, we study the cloud-radiative impact of high-level clouds on the present-day climate. We compare simulations with and without active radiative heating of high-level clouds, and we further perform simulations in which the radiative heating of all clouds is disabled.

We show that the radiative interactions of high-level clouds warm the entire troposphere, similarly to Lohmann and Roeckner (1995). The temperature impact is strongest in the tropical upper troposphere. High-level clouds strengthen the extratropical eddy-driven jet streams of both hemispheres, consistent with enhanced meridional temperature gradients in the upper troposphere. High-level clouds dominate the radiative impact of all clouds on the jet strength in the Northern Hemisphere. In the Southern Hemisphere, the jet strengthening by high-level clouds is overcompensated by an even stronger weakening effect from other clouds, indicating a competition between upper-tropospheric clouds and boundary-layer clouds (Voigt et al., 2023). High-level clouds dominate the overall cloud impact responsible for a decrease in tropical precipitation. However, they have no significant impact on the ITCZ position and Hadley cell strength.

We note three caveats of our study that create possibilities for follow-up studies. First, the ICON-ESM model used in our study underestimates the radiative heating of high-level clouds in the tropics compared to CERES-CALIPSO-CloudSat-MODIS satellite retrievals. This suggests that the impact of high-level clouds in the real world and in other models might be larger; it would therefore be interesting to test our results in other models. Second, turning off the cloud radiative heating, as done in our study, leads to small but still undesired surface temperature changes. To better focus on the cloud-radiative heating and cooling within the atmosphere, future studies could follow the recommendation of Harrop et al. (2023) and use all-sky surface radiative fluxes in simulations with transparent clouds, as this could reduce surface temperature changes. Third, our definition of high-level clouds includes clouds that extend into the lower troposphere. We expect that this downward extension would be substantially reduced in models with finer horizontal grid spacing, suggesting that such models would allow for a more precise quantification of the climate impacts of high-level clouds.

Independent of these caveats, our results confirm that radiative interactions of high-level clouds are important for climate. This emphasizes the need for a better representation of the radiative heating of high-level clouds in models.

# 7 Open Research

The ICON-ESM simulation output is archived in the Zenodo repository under `https://doi.org/10.5281/zenodo.10534120`. Upon acceptance of this manuscript, the simulation runscripts and Python scripts used to create all figures and tables are available in the GitLab server of the University of Vienna under `https://gitlab.phaidra.org/climate/haslehner-et-al-high-crh-jgr2024` and will be archived in the Zenodo repository.

A copy of the ICON-ESM model code can be obtained from `https://code.mpimet.mpg.de/projects/iconpublic`. The git commit of the ICON-ESM model with the diagice module, which allows to diagnose the radiative heating of high-level clouds, is 1f8253c5 (`https://gitlab.phaidra.org/climate/icon-esm-univie/-/commit/1f8253c5d708b89330f2007c510793f05f8c73a6`).

The CloudSat-CALIPSO derived ice water content from (J.-L. F. Li et al., 2012) is obtainable under `https://zenodo.org/records/3879566`. We used the CCCM cloud radiative heating estimate from (Ham et al., 2017), which is calculated using data from CCCM products, available from the Atmospheric Science Data Center data (`https://eosweb.larc.nasa.gov/project/CERES/CER_CCCM_Aqua-FM3-MODIS-CAL-CS_RelD1`).

During the review process, the runscripts and Python scripts used to create the figures and tables are available under `https://zenodo.org/records/10547145?token=e`

`yJhbGciOiJIUzUxMiJ9.eyJpZCI6IjQwNmI5YTU0LTY3ZDctNDg4Ny04MWVkLWI5Y2ZmZDYyM`
`TE1MCIsImRhdGEiOnt9LCJyYW5kb20iOiIyNGEwOGIOOWJkNDJiYjI1NDA0ZGFlYTA0NmNmM`
`GQONyJ9.rcHihMZKkQomo3jji-v1Wya8Ox6U347AFSzbbIwiVASiUAU_11lJSO3b8Vxk_hlX`
`BnOIrIk1SflOOekcoiQ3wg`.

# References

Albern, N., Voigt, A., Buehler, S. A., & Grützun, V. (2018). Robust and Nonrobust Impacts of Atmospheric Cloud-Radiative Interactions on the Tropical Circulation and Its Response to Surface Warming. *Geophysical Research Letters*, *45*(16), 8577-8585. `https://agupubs.onlinelibrary.wiley.com/doi/abs/10.1029/2018GL079599` doi: https://doi.org/10.1029/2018GL079599

Barnes, E. A., & Polvani, L. (2013). Response of the Midlatitude Jets, and of Their Variability, to Increased Greenhouse Gases in the CMIP5 Models. *Journal of Climate*, *26*(18), 7117 - 7135. `https://journals.ametsoc.org/view/journals/clim/26/18/jcli-d-12-00536.1.xml` doi: 10.1175/JCLI-D-12-00536.1

Butler, A. H., Thompson, D. W. J., & Heikes, R. (2010). The Steady-State Atmospheric Circulation Response to Climate Change–like Thermal Forcings in a Simple General Circulation Model. *Journal of Climate*, *23*(13), 3474 - 3496. `https://journals.ametsoc.org/view/journals/clim/23/13/2010jcli3228.1.xml` doi: https://doi.org/10.1175/2010JCLI3228.1

Cesana, G., Waliser, D. E., Henderson, D., L'Ecuyer, T. S., Jiang, X., & Li, J.-L. F. (2019). The Vertical Structure of Radiative Heating Rates: A Multimodel Evaluation Using A-Train Satellite Observations. *Journal of Climate*, *32*(5), 1573 - 1590. `https://journals.ametsoc.org/view/journals/clim/32/5/jcli-d-17-0136.1.xml` doi: https://doi.org/10.1175/JCLI-D-17-0136.1

Dinh, T., Gasparini, B., & Bellon, G. (2023). Clouds and Radiatively Induced Circulations. In *Clouds and their Climatic Impacts* (p. 239-253). American Geophysical Union (AGU). `https://agupubs.onlinelibrary.wiley.com/doi/abs/10.1002/9781119700357.ch11` doi: https://doi.org/10.1002/9781119700357.ch11

Dixit, V., Geoffroy, O., & Sherwood, S. C. (2018). Control of ITCZ Width by Low-Level Radiative Heating From Upper-Level Clouds in Aquaplanet Simulations. *Geophysical Research Letters*, *45*(11), 5788-5797. `https://agupubs.onlinelibrary.wiley.com/doi/abs/10.1029/2018GL078292` doi: https://doi.org/10.1029/2018GL078292

Gasparini, B., McGraw, Z., Storelvmo, T., & Lohmann, U. (2020). To what extent can cirrus cloud seeding counteract global warming? *Environmental Research Letters*, *15*(5), 054002.

Gasparini, B., Münch, S., Poncet, L., Feldmann, M., & Lohmann, U. (2017). Is increasing ice crystal sedimentation velocity in geoengineering simulations a good proxy for cirrus cloud seeding? *Atmospheric Chemistry and Physics*, *17*(7), 4871–4885. `https://acp.copernicus.org/articles/17/4871/2017/` doi:

508  10.5194/acp-17-4871-2017

509  Gasparini, B., Sokol, A. B., Wall, C. J., Hartmann, D. L., & Blossey, P. N.    (2022).
510      Diurnal Differences in Tropical Maritime Anvil Cloud Evolution.        *Journal*
511      *of Climate*, *35*(5), 1655 - 1677.        `https://journals.ametsoc.org/view/`
512      `journals/clim/35/5/JCLI-D-21-0211.1.xml`    doi: https://doi.org/10.1175/
513      JCLI-D-21-0211.1

514  Gryspeerdt, E., Quaas, J., Goren, T., Klocke, D., & Brueck, M.    (2018).    An auto-
515      mated cirrus classification.    *Atmospheric Chemistry and Physics*, *18*(9), 6157–
516      6169.    `https://acp.copernicus.org/articles/18/6157/2018/`        doi: 10
517      .5194/acp-18-6157-2018

518  Ham, S.-H., Kato, S., Rose, F. G., Winker, D., L'Ecuyer, T., Mace, G. G., . . .
519      Miller, W. F.    (2017).    Cloud occurrences and cloud radiative effects (CREs)
520      from CERES-CALIPSO-CloudSat-MODIS (CCCM) and CloudSat radar-lidar
521      (RL) products.    *Journal of Geophysical Research: Atmospheres*, *122*(16), 8852-
522      8884.        `https://agupubs.onlinelibrary.wiley.com/doi/abs/10.1002/`
523      `2017JD026725`    doi: https://doi.org/10.1002/2017JD026725

524  Harrop, B. E., & Hartmann, D. L.    (2016).    The Role of Cloud Radiative Heating in
525      Determining the Location of the ITCZ in Aquaplanet Simulations.    *Journal of*
526      *Climate*, *29*(8), 2741 - 2763.    `https://journals.ametsoc.org/view/journa`
527      `ls/clim/29/8/jcli-d-15-0521.1.xml`    doi: 10.1175/JCLI-D-15-0521.1

528  Harrop, B. E., Lu, J., Leung, L. R., Lau, W. K. M., Kim, K.-M., Medeiros, B.,
529      . . . Singh, B.    (2023).    An overview of cloud-radiation denial experiments
530      for the Energy Exascale Earth System Model version 1.        *EGUsphere*,
531      *2023*, 1–36.        `https://egusphere.copernicus.org/preprints/2023/`
532      `egusphere-2023-1555/`    doi: 10.5194/egusphere-2023-1555

533  Harrop, B. E., Lu, J., Liu, F., Garuba, O. A., & Leung, L. R.    (2018).    Sensitivity
534      of the ITCZ Location to Ocean Forcing Via Q-Flux Green's Function Ex-
535      periments.    *Geophysical Research Letters*, *45*(23), 13,116-13,123.    `https://`
536      `agupubs.onlinelibrary.wiley.com/doi/abs/10.1029/2018GL080772`    doi:
537      https://doi.org/10.1029/2018GL080772

538  Hartmann, D. L., Gasparini, B., Berry, S. E., & Blossey, P. N.    (2018).    The Life
539      Cycle and Net Radiative Effect of Tropical Anvil Clouds.    *Journal of Advances*
540      *in Modeling Earth Systems*, *10*(12), 3012-3029.    `https://agupubs.onlinelib`
541      `rary.wiley.com/doi/abs/10.1029/2018MS001484`    doi: https://doi.org/10
542      .1029/2018MS001484

543  Haslehner, K.    (2023).    *Cloud Radiative Effects of High-Level Clouds and their*
544      *Impact on Climate* (Master's thesis, University of Vienna, Vienna).    doi:
545      10.25365/thesis.73726

546  Heymsfield, A. J., Krämer, M., Luebke, A., Brown, P., Cziczo, D. J., Franklin,
547      C., . . . Tricht, K. V.    (2017).    Cirrus Clouds.    *Meteorological Monographs*,
548      *58*, 2.1 - 2.26.        `https://journals.ametsoc.org/view/journals/amsm/`
549      `58/1/amsmonographs-d-16-0010.1.xml`        doi: https://doi.org/10.1175/
550      AMSMONOGRAPHS-D-16-0010.1

551  Hong, Y., Liu, G., & Li, J.-L. F.    (2016).    Assessing the Radiative Effects of Global
552      Ice Clouds Based on CloudSat and CALIPSO Measurements.    *Journal of Cli-*
553      *mate*, *29*(21), 7651 - 7674. `https://journals.ametsoc.org/view/journals/`
554      `clim/29/21/jcli-d-15-0799.1.xml`    doi: 10.1175/JCLI-D-15-0799.1

555  Johansson, E., Devasthale, A., Tjernström, M., Ekman, A. M. L., Wyser, K., &
556      L'Ecuyer, T.    (2021).    Vertical structure of cloud radiative heating in the trop-
557      ics: confronting the EC-Earth v3.3.1/3P model with satellite observations.
558      *Geoscientific Model Development*, *14*(6), 4087–4101.    `https://gmd.copernicu`
559      `s.org/articles/14/4087/2021/`    doi: 10.5194/gmd-14-4087-2021

560  Jungclaus, J. H., Lorenz, S. J., Schmidt, H., Brovkin, V., Brüggemann, N.,
561      Chegini, F., . . . Claussen, M.    (2022).    The ICON Earth System Model
562      Version 1.0.        *Journal of Advances in Modeling Earth Systems*, *14*(4),

e2021MS002813. https://agupubs.onlinelibrary.wiley.com/doi/
abs/10.1029/2021MS002813 (e2021MS002813 2021MS002813) doi:
https://doi.org/10.1029/2021MS002813

Järvinen, E., van Diedenhoven, B., Magee, N., Neshyba, S., Schnaiter, M., Xu, G.,
... Kato, S. (2023). Ice Crystal Complexity and Link to the Cirrus Cloud
Radiative Effect. In *Clouds and their climatic impacts* (p. 47-85). American
Geophysical Union (AGU). https://agupubs.onlinelibrary.wiley.com/
doi/abs/10.1002/9781119700357.ch3 doi: https://doi.org/10.1002/
9781119700357.ch3

Kärcher, B. (2017). Cirrus Clouds and Their Response to Anthropogenic Activities.
*Current Climate Change Reports*, *3*(1), 45–57.

Kato, S., Ham, S.-H., Miller, W. F., Sun-Mack, S., Rose, F. G., Chen, Y., &
Mlynczak, P. E. (2021). *Variable Descriptions of the A-Train Integrated
CALIPSO, CloudSat, CERES, and MODIS Merged Product (CCCM or
C3M).* https://ceres.larc.nasa.gov/documents/collect_guide/pdf/
c3m_variables.RelD1.20211117.pdf

Kato, S., Rose, F. G., Rutan, D. A., Thorsen, T. J., Loeb, N. G., Doelling, D. R.,
... Ham, S.-H. (2018). Surface Irradiances of Edition 4.0 Clouds and
the Earth's Radiant Energy System (CERES) Energy Balanced and Filled
(EBAF) Data Product. *Journal of Climate*, *31*(11), 4501 - 4527. https://
journals.ametsoc.org/view/journals/clim/31/11/jcli-d-17-0523.1.xml
doi: https://doi.org/10.1175/JCLI-D-17-0523.1

Krämer, M., Rolf, C., Spelten, N., Afchine, A., Fahey, D., Jensen, E., ... Sourdeval,
O. (2020). A microphysics guide to cirrus – Part 2: Climatologies of clouds
and humidity from observations. *Atmospheric Chemistry and Physics*, *20*(21),
12569–12608. https://acp.copernicus.org/articles/20/12569/2020/ doi:
10.5194/acp-20-12569-2020

Lauer, A., Bock, L., Hassler, B., Schröder, M., & Stengel, M. (2023). Cloud Clima-
tologies from Global Climate Models—A Comparison of CMIP5 and CMIP6
Models with Satellite Data. *Journal of Climate*, *36*(2), 281 - 311. https://
journals.ametsoc.org/view/journals/clim/36/2/JCLI-D-22-0181.1.xml
doi: https://doi.org/10.1175/JCLI-D-22-0181.1

Lawson, R. P., Woods, S., Jensen, E., Erfani, E., Gurganus, C., Gallagher, M., ...
Krämer, M. (2019). A Review of Ice Particle Shapes in Cirrus formed In
Situ and in Anvils. *Journal of Geophysical Research: Atmospheres*, *124*(17-
18), 10049-10090. https://agupubs.onlinelibrary.wiley.com/doi/abs/
10.1029/2018JD030122 doi: https://doi.org/10.1029/2018JD030122

Li, J.-L. F., Waliser, D. E., Chen, W.-T., Guan, B., Kubar, T., Stephens, G., ...
Horowitz, L. (2012). An observationally based evaluation of cloud ice wa-
ter in CMIP3 and CMIP5 GCMs and contemporary reanalyses using con-
temporary satellite data. *Journal of Geophysical Research: Atmospheres*,
*117*(D16). https://agupubs.onlinelibrary.wiley.com/doi/abs/10.1029/
2012JD017640 doi: https://doi.org/10.1029/2012JD017640

Li, Y., Thompson, D. W. J., & Bony, S. (2015). The Influence of Atmospheric Cloud
Radiative Effects on the Large-Scale Atmospheric Circulation. *Journal of Cli-
mate*, *28*(18), 7263 - 7278. https://journals.ametsoc.org/view/journals/
clim/28/18/jcli-d-14-00825.1.xml doi: 10.1175/JCLI-D-14-00825.1

Loeb, N. G., Doelling, D. R., Wang, H., Su, W., Nguyen, C., Corbett, J. G.,
... Kato, S. (2018). Clouds and the Earth's Radiant Energy System
(CERES) Energy Balanced and Filled (EBAF) Top-of-Atmosphere (TOA)
Edition-4.0 Data Product. *Journal of Climate*, *31*(2), 895 - 918. https://
journals.ametsoc.org/view/journals/clim/31/2/jcli-d-17-0208.1.xml
doi: https://doi.org/10.1175/JCLI-D-17-0208.1

Lohmann, U., & Roeckner, E. (1995). Influence of cirrus cloud radiative forcing on
climate and climate sensitivity in a general circulation model. *Journal of Geo-*

*physical Research: Atmospheres*, *100*(D8), 16305-16323. `https://agupubs.onl` `inelibrary.wiley.com/doi/abs/10.1029/95JD01383` doi: https://doi.org/ 10.1029/95JD01383

Lohmann, U., & Roeckner, E. (1996). Design and performance of a new cloud micro-physics scheme developed for the ECHAM general circulation model. *Climate Dynamics*, *12*, 557–572.

L'Ecuyer, T. S., Hang, Y., Matus, A. V., & Wang, Z. (2019). Reassessing the Effect of Cloud Type on Earth's Energy Balance in the Age of Active Spaceborne Observations. Part I: Top of Atmosphere and Surface. *Journal of Climate*, *32*(19), 6197 - 6217. `https://journals.ametsoc.org/view/` `journals/clim/32/19/jcli-d-18-0753.1.xml` doi: https://doi.org/10.1175/ JCLI-D-18-0753.1

Matus, A. V., & L'Ecuyer, T. S. (2017). The role of cloud phase in Earth's radiation budget. *Journal of Geophysical Research: Atmospheres*, *122*(5), 2559-2578. `https://agupubs.onlinelibrary.wiley.com/doi/abs/10.1002/2016J` `D025951` doi: https://doi.org/10.1002/2016JD025951

Morrison, H., van Lier-Walqui, M., Fridlind, A. M., Grabowski, W. W., Harrington, J. Y., Hoose, C., ... Xue, L. (2020). Confronting the Challenge of Modeling Cloud and Precipitation Microphysics. *Journal of Advances in Modeling Earth Systems*, *12*(8), e2019MS001689. `https://agupubs.onlinelibrary.wiley.c` `om/doi/abs/10.1029/2019MS001689` (e2019MS001689 2019MS001689) doi: https://doi.org/10.1029/2019MS001689

Oreopoulos, L., Cho, N., & Lee, D. (2017). New insights about cloud vertical structure from CloudSat and CALIPSO observations. *Journal of Geophysical Research: Atmospheres*, *122*(17), 9280-9300. `https://agupubs.onlinelibrary` `.wiley.com/doi/abs/10.1002/2017JD026629` doi: https://doi.org/10.1002/ 2017JD026629

Pendergrass, A. G., & Hartmann, D. L. (2014). The Atmospheric Energy Constraint on Global-Mean Precipitation Change. *Journal of Climate*, *27*(2), 757 - 768. `https://journals.ametsoc.org/view/journals/clim/27/2/jcli-d-13` `-00163.1.xml` doi: https://doi.org/10.1175/JCLI-D-13-00163.1

Pincus, R., & Stevens, B. (2013). Paths to accuracy for radiation parameterizations in atmospheric models. *Journal of Advances in Modeling Earth Systems*, *5*(2), 225-233. `https://agupubs.onlinelibrary.wiley.com/doi/abs/10.1002/ja` `me.20027` doi: https://doi.org/10.1002/jame.20027

Ruppert, J. H., Wing, A. A., Tang, X., & Duran, E. L. (2020). The critical role of cloud–infrared radiation feedback in tropical cyclone development. *Proceedings of the National Academy of Sciences*, *117*(45), 27884-27892. `https://www.pna` `s.org/doi/abs/10.1073/pnas.2013584117` doi: 10.1073/pnas.2013584117

Stevens, B., Bony, S., & Webb, M. (2012). *Clouds On-Off Klimate Intercomparison Experiment (COOKIE).*

Sundqvist, H., Berge, E., & Kristjánsson, J. E. (1989). Condensation and Cloud Parameterization Studies with a Mesoscale Numerical Weather Prediction Model. *Monthly Weather Review*, *117*(8), 1641 - 1657. `https://journals.ametsoc.o` `rg/view/journals/mwre/117/8/1520-0493_1989_117_1641_cacpsw_2_0_co_2` `.xml` doi: 10.1175/1520-0493(1989)117⟨1641:CACPSW⟩2.0.CO;2

Tiedtke, M. (1989). A comprehensive mass flux scheme for cumulus parameterization in large-scale models. *Monthly Weather Review*, *117*(8), 1779–1800.

Voigt, A., & Albern, N. (2019). No Cookie for Climate Change. *Geophysical Research Letters*, *46*(24), 14751-14761. `https://agupubs.onlinelibrary.w` `iley.com/doi/abs/10.1029/2019GL084987` doi: https://doi.org/10.1029/ 2019GL084987

Voigt, A., Albern, N., Ceppi, P., Grise, K., Li, Y., & Medeiros, B. (2021). Clouds, radiation, and atmospheric circulation in the present-day climate and under climate change. *WIREs Climate Change*, *12*(2), e694.

https://wires.onlinelibrary.wiley.com/doi/abs/10.1002/wcc.694
doi: https://doi.org/10.1002/wcc.694

Voigt, A., Albern, N., & Papavasileiou, G. (2019). The Atmospheric Pathway of the Cloud-Radiative Impact on the Circulation Response to Global Warming: Important and Uncertain. *Journal of Climate*, *32*(10), 3051–3067.

Voigt, A., North, S., Gasparini, B., & Ham, S.-H. (2023). Atmospheric cloud-radiative heating in CMIP6 and observations, and its response to surface warming. *EGUsphere*, *2023*, 1–31. https://egusphere.copernicus.org/preprints/2023/egusphere-2023-2612/ doi: 10.5194/egusphere-2023-2612

Voigt, A., & Shaw, T. A. (2016). Impact of Regional Atmospheric Cloud Radiative Changes on Shifts of the Extratropical Jet Stream in Response to Global Warming. *Journal of Climate*, *29*(23), 8399 - 8421. https://journals.ametsoc.org/view/journals/clim/29/23/jcli-d-16-0140.1.xml doi: 10.1175/JCLI-D-16-0140.1

Watt-Meyer, O., & Frierson, D. M. W. (2017). Local and Remote Impacts of Atmospheric Cloud Radiative Effects Onto the Eddy-Driven Jet. *Geophysical Research Letters*, *44*(19), 10,036-10,044. https://agupubs.onlinelibrary.wiley.com/doi/abs/10.1002/2017GL074901 doi: https://doi.org/10.1002/2017GL074901

Webb, M. J., Andrews, T., Bodas-Salcedo, A., Bony, S., Bretherton, C. S., Chadwick, R., ... others (2017). The Cloud Feedback Model Intercomparison Project (CFMIP) contribution to CMIP6. *Geoscientific Model Development*, *10*(1), 359–384.

Wernli, H., Boettcher, M., Joos, H., Miltenberger, A. K., & Spichtinger, P. (2016). A trajectory-based classification of ERA-Interim ice clouds in the region of the North Atlantic storm track. *Geophysical Research Letters*, *43*(12), 6657-6664. https://agupubs.onlinelibrary.wiley.com/doi/abs/10.1002/2016GL068922 doi: https://doi.org/10.1002/2016GL068922

Wilks, D. S. (2016). "The Stippling Shows Statistically Significant Grid Points": How Research Results are Routinely Overstated and Overinterpreted, and What to Do about It. *Bulletin of the American Meteorological Society*, *97*(12), 2263 - 2273. https://journals.ametsoc.org/view/journals/bams/97/12/bams-d-15-00267.1.xml doi: https://doi.org/10.1175/BAMS-D-15-00267.1